Temporal expression profiles of lncRNA and mRNA in human embryonic stem cell-derived motor neurons during differentiation

Xue-Jiao Sun[1], Ming-Xing Li[1], Chen-Zi Gong[1], Jing Chen[1], Mohammad Nasb[1], Sayed Zulfiqar Ali Shah[1], Rehan Muhammad[1], Ya-Jie Li[1], Hong Chen[1],*

[1] Department of Rehabilitation Medicine, Tongji Hospital, Tongji Medical College, Huazhong University of Science and Technology, Wuhan, China

*Corresponding Author:
Hong Chen
1095 Jiefang Road, Wuhan 430030, China.
Email address: chenhong1129@hotmail.com

Abstract

Background: Human embryonic stem cells (hESC) are an invaluable research tool to study motor neuron development and disorders. However, transcriptional regulation of multiple temporal stages from ESCs to spinal motor neurons (MNs) has not yet been fully elucidated. Thus, the goals of this study were to profile the time-course expression patterns of lncRNAs during MN differentiation of ESCs and to clarify the potential mechanisms of the lncRNAs that are related to MN differentiation.

Methods: We utilized our previous protocol which can harvest motor neuron in more than 90% purity from hESCs. Then, differentially expressed lncRNAs (DElncRNAs) and mRNAs (DEmRNAs) during MN differentiation were identified through RNA sequencing. Bioinformatic analyses were performed to assess potential biological functions of genes. We also performed qRT-PCR to validate the DElncRNAs and DEmRNAs.

Results: Total 441 lncRNAs and 1068 mRNAs at day 6, 443 and 1175 at day 12, and 338 lncRNAs and 68 mRNAs at day 18 were differentially expressed compared with day 0. Bioinformatic analyses identified that several key regulatory genes including POU5F1, TDGF1, SOX17, LEFTY2 and ZSCAN10, which involved in the regulation of embryonic development. We also predicted 283 target genes of DElncRNAs, in which 6 mRNAs were differentially expressed. Significant fold changes in lncRNAs (NCAM1-AS) and mRNAs (HOXA3) were confirmed by qRT-PCR. Then, through predicted overlapped miRNA verification, we constructed lncRNA NCAM1-AS-miRNA-HOXA3 network.

39 **Conclusion:** This study comprehensively identified lncRNAs and mRNAs during MN
40 differentiation of hESCs, providing a theoretical basis for further study of the regulatory role of
41 lncRNAs in MN differentiation.
42
43 **Keyword**s: Embryonic stem cells; Long non-coding RNA; Motor neuron; Differentiation; RNA
44 sequencing
45

Introduction

47 Generation of specific cell types from hESCs in vitro have provided powerful platforms to study
48 human disease and to understand fundamental biological processes. Highly efficient directed
49 differentiation of hESCs into spinal motor neurons have been used to explore not only MN
50 development but also MN disorders mechanism [1, 2]. Motor neurons are responsible for
51 innervating skeletal muscles in the periphery and controlling movement. Transcription factors
52 (TFs) regulate precise temporal and spatial gene expression in motor neuron specification and
53 differentiation [3, 4]. The TFs Olig2 and Ngn2 function in opposition to regulate gene expression
54 in MN progenitors in the pMN domain and the TFs Isl1 and Lhx3 are crucial for specifying MN
55 identity [5-7].
56   LncRNAs, ranging in length from 200 nt to 100 kb, are highly expressed in the central nervous
57 system. Accumulating evidence suggested that lncRNA played crucial roles in numerous
58 biological and pathological processes at the chromatin remodeling level, transcriptional level and
59 post-transcriptional level [8, 9]. Notably, lncRNAs function as key regulators of cell
60 differentiation and development, especially in neurogenesis. Particularly, lncRNAs can regulate
61 ESC pluripotency and control multiple lineage differentiation by association with miRNAs,
62 RNA-binding proteins, and epigenetic modifiers [10]. LncRNA-1604 functioned as competing
63 endogenous RNAs (ceRNAs) of miR-200c and indirectly regulated the core TFs ZEB1 and
64 ZEB2 during neural differentiation from mouse ESCs [11]. LncRNA Haunt functions as a
65 genetic enhancer and an epigenetic repressor of HOXA gene activation during ESC
66 differentiation [12]. *Dlk1-Dio3* locus-derived lncRNAs play a critical role in maintaining
67 postmitotic MN cell fate by repressing progenitor genes and they shape MN subtype identity by
68 regulating Hox genes [13]. Nevertheless, at present very little functional characterization of
69 lncRNAs in human motor neuron differentiation has been elucidated.
70   We used spinal motor neuron differentiation to profile the temporal changes without further
71 purification steps. We combined highly efficient MN differentiation of hESCs in vitro with
72 RNA-seq analysis to reveal the expression profiles of lncRNAs and mRNAs. Our findings may
73 provide a new theoretical basis for further studies on lncRNAs modulation of motor neuron
74 differentiation.

Materials and Methods

Cell cultures form embryonic stems cells to spinal motor neurons

H9 (WA09, NIH registry 0046) hESC lines were obtained from WiCell Research Institute (Madison, WI). Human ESCs were maintained on irradiated mouse embryonic fibroblasts and differentiated as described before [2]. Briefly, ESCs were cultured using MN differentiation medium containing DMEM/F12, Neurobasal medium, N2, B27, ascorbic acid, Glutamax and penicillin/streptomycin (All from Gibco). The medium was additionally supplemented with chemical compounds: 3 μM CHIR99021 (Torcris), 2 μM DMH-1 (Torcris) and 2 μM SB431542 (Stemgent) for 6 days differentiated into neuroepithelial progenitors; 1 μM CHIR99021, 2 μM DMH-1, and 2 μM SB431542, 0.1 μM RA (Sigma) and 0.5 μM Purmorphamine (Pur, Sigma) for 6 days differentiated into MN progenitors; 0.5 μM RA and 0.1μM Purmorphamine for 6 days differentiated into MNs.

Total RNA isolation and RNA sequencing

Total RNA from samples was extracted using the Trizol reagent (Invitrogen). RNA quantity and purity of total were confirmed using NanoDrop ND-2000 spectrophotometer (Thermo Fisher Scientific, USA). RNA integrity was assessed by Agilent 2100 Bioanalyzer (Agilent Technologies, USA). Ribosomal RNA was removed. Sequencing libraries were constructed. The dTTP were replaced by dUTP in the reaction buffer during second strand cDNA synthesis. Products were purified and library quality was assessed on the Agilent Bioanalyzer 2100 system. RNA Sequencing was performed on the Illumina HiSeq ((Illumina, USA) by KangChen Biotechnology Corporation (Shanghai, China) using next-generation sequencing analysis. Raw data of the RNA sequencing have been deposited in the Gene Expression Omnibus (GEO) public database (accession number: GSE151744).

Immunocytochemistry

The primary antibodies information was used: SOX1 (gIgG, 1:1000, R&D), HOXA3 (mIgG, 1:1000, R&D), OLIG2 (rIgG, 1:1000, Millipore), HB9 (rIgG, 1:1000, Millipore), NF-200 (mIgG, 1:400, CST). Image J was used to perform cell counting (NIH, USA).

Quantitative real-time PCR

Total RNA was extracted using the Trizol reagent (Invitrogen). qRT-PCR was then performed and the $2^{-\Delta\Delta Ct}$ method was calculated for quantification. The GAPDH was used as an internal control. The primer sequences used are listed in Table 1.

Transfection of lncRNA Smart Silencer

Motor neuron progenitors were transfected with lncRNA Smart Silencer (RiboBio Co., Guangzhou, China) to knock down the expression of NCM1-AS. The lncRNA Smart Silencer contained a mixture of three siRNAs and three antisense oligonucleotides. The target siRNA sequences were as followed: 5'-ACAACCCGATGACAGCAGA-3', 5'-

115   CCAAATGGAGAACGTGCAA-3' and 5'-GTACTCGGTCTTTGCTGGC-3'. The target
116   antisense oligonucleotides sequence were as followed: 5'-ATGAAAGGAAAGGCACCAGC-3',
117   5'-ACATCTAACAAGGAGGACAC-3', 5'-AGGTTGACCGCAATGCACAT-3'. The negative
118   control (NC) Smart Silencer did not contain domains sequences homologous to those of humans,
119   rats, or mice. The cells were transfected with the lncRNA Smart silencer using Lipofectamine
120   3000 (Invitrogen, USA) and collected 48 hours after transfection for RNA isolation.
121

122   **Bioinformatic analysis**
123   Gene Ontology (GO) analysis was used to investigate differentially expressed mRNAs with GO
124   categories. The predicted target genes above were conducted using the DAVID database
125   (http://david.abcc.ncifcrf.gov/). GO terms with a *P* value < 0.05 were considered as significantly
126   enriched. PPI networks was used STRING database (https://string-db.org/) and Cytoscape. The
127   networks were visualized in CytoHubb plug-in of Cytoscape. LncRNAs and mRNAs possessing
128   microRNA recognition elements (MREs) for the targeted miRNAs were predicted using the
129   miRanda and TargetScan.
130

131   **Statistical analysis**
132   All qRT-PCR results are expressed as the means ± SEM of at least three independent
133   experiments. Statistical analyses were performed with SPSS statistics software version 22.0. P
134   values < 0.05 was considered statistically significant. All graphs were made with GraphPad
135   Prism 8.
136

Results

Differentiation of high purity motor neuron from human embryonic stem cells

In this study, we used hESCs to differentiate into spinal cord MNs in vitro. The MNs were generated using chemical protocol described as method part [2] (Figure 1A). The hESCs can differentiate into SOX1 neuroepithelial progenitors at day 6, OLIG2 motor neuron progenitors at day 12, and HB9 motor neuron at day 18 high efficiently by using a combination of small molecules (Figure 1B-D).

Patterns of gene expression changes from hESCs to motor neuron

High throughput sequencing is an efficient approach for investigating the biological function of RNAs. All the differently expressed DElncRNAs and DElncRNAs were statistically significant ($P < 0.05$) with fold change (FC) > 2.

A total of 441 DElncRNAs (192 up-regulated and 249 down-regulated), 443 DElncRNAs (198 up-regulated and 245 down-regulated) and 338 DElncRNAs (164 up-regulated and 174 down-regulated) were identified in D6 *vs* D0 (neuroepithelial progenitors, NEP), D12 *vs* D0 (motor neuron progenitors, MNP), and D18 *vs* D0 (motor neuron, MN) respectively (Additional file 1). The volcano plots of expression profile for all the detected transcripts showed the relationship between the fold change and the significance (Figure 2A-C). To determine the key RNAs in human MN differentiation, we analyzed DElncRNAs in Venn diagram form. Veen analysis revealed that 33 lncRNAs were simultaneously up regulated and 78 were down regulated on D6, D12 and D18 (Figure 2D-E). Meanwhile, a total of 1068 DEmRNAs (360 up-regulated and 708 down-regulated), 1175 mRNAs (444 up-regulated and 731 down-regulated) and 68 DEmRNAs (34 up-regulated and 34 down-regulated) were identified in D6 *vs* D0, D12 *vs* D0 and D18 *vs* D0 respectively (Additional file 2). The volcano plots was shown in Figure 3A-C. Veen analysis revealed that 8 mRNAs were simultaneously up-regulated and 34 down-regulated (Figure 3D-E).

Validation of lncRNAs and mRNAs expression

To verify the results of the RNA sequencing, five strongly expressed DElncRNAs and DEmRNAs during MN differentiation with FC＞40 were selected for qRT-PCR validation. As shown in Figure 4A-E, the expression of ZSCAN10, OCT4 and VRTN were down regulated, while HOXA3 and SP9 were up regulated. Moreover, the expression of ENST00000454596 (lncRNA rp11.001), ENST00000419695 (lncRNA rp11.003) and ENST00000583521 (lncRNA rp11-c9-001) were down regulated, while NCAM1-AS were up regulated (Figure 4F-J). However, lncRNA H19 increased at D12, but decreased significantly at D18. Our results agreed with the data of RNA-sequencing generally.

Bioinformatics analysis during MN differentiation

To identify the key factors that regulated MN differentiation, GO analysis of DEmRNAs was performed on three different aspects namely biological process (BP), molecular function (MF) and cellular component (CC) shown in Figure 5A. In the BP domain, the top 6 GO terms were

177 enriched in cell migration involved in gastrulation, somatic stem cell population maintenance,
178 positive regulation of transcription from RNA polymerase II promoter, positive regulation of cell
179 proliferation, cardiac cell fate determination and anterior/posterior pattern specification. Genes
180 associated with cell migration involved in gastrulation were SOX17, MIXL1 and CER1. Genes
181 associated with positive regulation of cell proliferation were EPHA1, ETS1, HOXA3, POU3F3,
182 FLT1, and TDGF1. In the CC domain, the top 3 GO terms were transcription factor complex,
183 membrane raft and nucleoplasm. In the MF domain, the top 3 GO terms were sequence-specific
184 DNA binding, transcription factor activity and HMG box domain binding. Figure 5B showed the
185 heat map of DEmRNAs.
186   Furthermore, the Protein-Protein Interaction (PPI) network of DEmRNAs contained 28 nodes
187 and 39 edges (Figure 5C). The topological analysis of the network was carried out by Network
188 Analyzer in Cytoscape. PPI network was imported into Cytohubba to determine the hub
189 transcription factors with high degree of connectivity between the nodes. The top ten hub genes
190 were POU5F1, TDGF1, SOX17, LEFTY2, ZSCAN10, CER1, ZFP42, MIXL1, L1TD1 and
191 ESRP1 shown in Figure 5C.
192
193 **Analysis of lncRNAs target mRNAs**
194 LncRNA may regulate nearby protein-coding genes by cis-regulatory effects. We analyzed
195 potential function of the target genes of DElncRNAs at D18 *vs* D0. Total 338 DElncRNAs had
196 289 mRNAs target genes (Additional file 3). Then we performed GO analysis on DElncRNAs
197 target genes to explore their potential biological functions. The GO terms related to BP, CC and
198 MF were shown in Figure 6A. The most enriched BP term was related to positive regulation of
199 telomerase activity. As for CC, we found that the most enriched term were nucleoplasm and
200 transcription factor complex. As for MF, transcription factor activity, sequence-specific DNA
201 binding and metal ion binding were most enriched. Moreover, KEGG analysis was made in
202 Figure 6B and the most enriched 5 top pathway terms were MAPK signaling pathway, Ribosome,
203 Pyrimidine metabolism, Hippo signaling pathway and Cushing syndrome. Veen diagram analysis
204 indicated that 6 mRNAs targeted by DElncRNAs were found at the interaction of DEmRNAs at
205 D18 *vs* D0 (Figure 6C). Moreover, lncRNAs and their *cis* target DEmRNAs were up-regulated at
206 D18, including two well-known TFs HOXA6 and HOXC9. We also performed the topological
207 analysis of PPI network on these target genes (Figure 7), indicating the highly connected hub
208 nodes in PPI network.
209
210 **Construction of lncRNA-miRNA-mRNA interaction network**
211 LncRNAs can regulate gene expression by acting as ceRNAs to sponge miRNAs [14].
212 Thererfore, we constructed a ceRNA interaction network from verified DE mRNAs and DE
213 lncRNAs based on previous qRT-PCR data. As the RNA sequencing and PCR data shown, the
214 transcription factors HOXA3 and SP9, exhibited continuous up-regulation in the transition from
215 ESCs to MN stages, and especially showed a sharp up-regulation coincident with MNs
216 specification. Interestingly, the expression of lncRNA NCAM1-AS showed same trend as

217   HOXA3 and SP9. The NCAM1-AS is antisense lncRNA with two exons, produced from gene
218   NCAM1, which is involved in cell adhesion, axonal outgrowth, synapse formation during
219   development and differentiation, and highly expressed in the developing central and peripheral
220   nervous systems [15]. Bioinformatics analysis of same putative target miRNAs of HOXA3 and
221   lncRNA NCAM1-AS identified a direct binding site of has-miR-338-3p. Thus, lncRNA-miRNA-
222   mRNA pathway was constructed including: lncRNA NCAM1-AS-miR-338-3p-HOXA3.
223   Moreover, the expression of HOXA3 was down-regulated at D12 in the NCAM1-AS Smart
224   Silencer group compared to NC group (Figure 8A). Furthermore, immunofluorescence analysis
225   showed a decreased expression of OLIG2 in the NCAM1-AS knockdown group (Figure 8B).
226   Therefore, the results suggested that lncRNA NCAM1-AS can affect MNP differentiation.
227
228

229   **Discussion**
230   Motor neuron differentiation is precisely regulated and orchestrated by combinatorial expression
231   of TFs during embryogenesis [4]. Accumulating evidence suggested that lncRNAs could interact
232   with transcription factors to regulate cell differentiation [16-18]. In this study, we profiled
233   mRNAs and lncRNAs expression from our highly efficient ESC-derived MN differentiation
234   protocol to study the development of MNs. Our analysis focused on the identification of
235   transcription factors and lncRNAs that are strongly involved in the temporal development of
236   MNs.
237   ESCs, derived from the inner cell mass of blastocyst stage embryos, can both self-renew and
238   differentiate into other cell types [19]. The balance between self-renewal and differentiation is
239   regulated by a complex interaction network of translation factors. Pluripotent genes such as
240   Oct4, Nanog, Sox2, Klf4, and Myc [20], activated in ESCs, were inhibited during cell
241   differentiation, whereas expression of differentiation marker genes increases gradually.
242   Notably, we found the well-known pluripotency-associated transcription factors POU5F1 (also
243   known as OCT4) and TDGF1 which were hub downstream-regulated genes upon MN
244   differentiation in our study. It has been reported that lincRNA linc-RoR, may function as a key
245   ceRNA to link the network of miRNAs and core TFs OCT4, SPX2, and NANOG, thus
246   regulating ESC maintenance and differentiation [21]. As a previous study [22], hub transcription
247   factor ZSCAN10, verified by qRT-PCR, also down-regulated in our study and could regulate
248   ESCs gene expression and differentiation. OCT4 can directly regulate expression of ZSCAN10
249   and TDGF1 [23, 24].
250   Here, we also identified *cis* regulatory target genes HOXA6 and HOXC9 of lncRNA HOXA-
251   AS3 and HOXC-AS2 at MN stage, respectively. Spinal MNs acquire specialized pool identities
252   that guide their axons to target muscles in the limb, and the specificity of these precise
253   connections[25]. MNs could express many HOX genes specifying MN pool identity and
254   connectivity [25, 26]. HOX6 paralog group genes (HOXA6, HOXC6, and HOXB6) contributed
255   to diverse aspects of motor neuron subtype differentiation, and determined lateral motor column
256   (LMC) fate at forelimb levels of the spinal cord [26]. In addition, HOXC9 determined thoracic

257 level MN population fates, including preganglionic column (PGC) and hypaxial motor column
258 (HMC) neurons [27]. The LncRNA HOXA-AS3 was found to inhibit osteogenic differentiation
259 and promote adipogenic differentiation [28]. The up-regulated lncRNAs HOXA-AS3 and
260 HOXC-AS2 at human MN derived from ESCs was first identified in our study. The two
261 lncRNAs might be involved in MN differentiation by *cis*-regulating HOXA6 and HOXC9, which
262 needs further study.
263   Our sequencing results suggested a series of mRNAs and lncRNAs significantly changed
264 during the transition from ESC to motor neurons. HOXA3, SP9 and lncRNA NCAM1-AS
265 verified by PCR were observed dramatically up-regulated, especially at period of motor neuron.
266 HOXA3 and HOXB3 are necessary for the specification of Pax6-and Olig2-dependent somatic
267 MN progenitors [29]. In addition, HOX1 was reported to be involved in mediating both the role
268 of RA-signaling in specification of hindbrain MNs [30]. In our sequencing data, HOXB3 was up-
269 regulated at NEP and MNP stages but not altered at MN stage. The neuronal differentiation
270 marker NCAM was involved in motor neurons functionally expanding synaptic territory [31].
271   Additionally, the potential function of lncRNA NCAM1-AS has been originally identified in
272 human MN differentiation from ESC. The lncRNAs could function as miRNA sponges and
273 might compete against other endogenous RNAs to regulate mRNA expression levels and
274 maintain normal biological function. Bioinformatics analysis indicated lncRNA-miRNA-mRNA
275 pathway: lncRNA NCAM1-AS-miR-338-3p-HOXA3. A recent study found that miR-338-3p
276 targeted and inhibited HOXA3 in breast cancer [32]. Thus, the upregulated lncRNA NCAM1-AS
277 might inhibit the expression of miRNA by acting as a miRNA sponge, and in turn, increasing the
278 expressions of MN differentiation-associated mRNAs HOXA3. The dysregulated lncRNAs may
279 regulate gene expression through many ways and play a critical role in the processes of neuronal
280 differentiation.
281

282 **Conclusions**
283 In conclusion, we utilized our highly efficient ESC-derived MNs differentiation protocol and
284 next-generation sequencing to provide new insights into understanding the molecular
285 mechanisms underlying MN differentiation and modulating lineage commitment of ESCs. The
286 understanding of MN differentiation could ultimately offer the early diagnosis and novel
287 therapeutic tools of MN-related diseases. More importantly, additional experiments will be
288 needed to further validate those lncRNAs functions.
289

290

Declarations

Acknowledgements

We acknowledge Professor Su-Chun Zhang of University of Wisconsin–Madison for his
assistance during the development of this work.

Competing interests

The authors declare that they have no competing interests.

Funding

This study was supported in part by the National Key Research and Development Project of
China (2016YFA0102500), the National Natural Science Foundation of China (81801066),
the China Postdoctoral Science Foundation (2018M640706).

Author contributions

Xue-Jiao Sun was responsible for assembly of data, data analysis and interpretation, and
manuscript writing. Ming-Xing Li and Chen-Zi Gong were responsible for the preliminary
data search, selection and manuscript revision; Jing Chen and Ya-Jie Li, collection of data
and data analysis. Mohammad Nasb, Sayed Zulfiqar Ali Shah and Rehan Muhammad were
responsible for manuscript revision. Hong Chen were responsible for conception, experiment
design and final approval of manuscript. All authors read and approval the final manuscript.

Author's information

Tongji Hospital, Tongji Medical College, Huazhong University of Science and Technology,
Jiefang Avenue 1095, Wuhan 430030, China.

316

Reference

318 1   Chen H, K Qian, Z Du, J Cao, A Petersen, H Liu, LWt Blackbourn, CL Huang, A Errigo,
319   Y Yin, J Lu, M Ayala, and SC Zhang. (2014). Modeling ALS with iPSCs reveals that
320   mutant SOD1 misregulates neurofilament balance in motor neurons. Cell Stem Cell **14**:
321   796-809.
322 2   Du ZW, H Chen, H Liu, J Lu, K Qian, CL Huang, X Zhong, F Fan, and SC Zhang.
323   (2015). Generation and expansion of highly pure motor neuron progenitors from human
324   pluripotent stem cells. Nat Commun **6**: 6626.
325 3   Cave C and S Sockanathan. (2018). Transcription factor mechanisms guiding motor
326   neuron differentiation and diversification. Curr Opin Neurobiol **53**: 1-7.
327 4   Alaynick WA, TM Jessell, and SL Pfaff. (2011). SnapShot: spinal cord development.
328   Cell **146**: 178-178 e1.
329 5   Thaler JP, SK Lee, LW Jurata, GN Gill, and SL Pfaff. (2002). LIM factor Lhx3
330   contributes to the specification of motor neuron and interneuron identity through cell-
331   type-specific protein-protein interactions. Cell **110**: 237-49.
332 6   Seo SY, B Lee, and S Lee. (2015). Critical Roles of the LIM Domains of Lhx3 in
333   Recruiting Coactivators to the Motor Neuron-Specifying Isl1-Lhx3 Complex. Mol Cell
334   Biol **35**: 3579-89.
335 7   Lee SK, B Lee, EC Ruiz, and SL Pfaff. (2005). Olig2 and Ngn2 function in opposition to
336   modulate gene expression in motor neuron progenitor cells. Genes Dev **19**: 282-94.
337 8   Mercer TR, ME Dinger, and JS Mattick. (2009). Long non-coding RNAs: insights into
338   functions. Nature Reviews Genetics **10**: 155-159.
339 9   Kopp F and JT Mendell. (2018). Functional Classification and Experimental Dissection
340   of Long Noncoding RNAs. Cell **172**: 393-407.
341 10   Loewer S, MN Cabili, M Guttman, YH Loh, K Thomas, IH Park, M Garber, M Curran, T
342   Onder, S Agarwal, PD Manos, S Datta, ES Lander, TM Schlaeger, GQ Daley, and JL
343   Rinn. (2010). Large intergenic non-coding RNA-RoR modulates reprogramming of
344   human induced pluripotent stem cells. Nat Genet **42**: 1113-7.
345 11   Weng R, C Lu, X Liu, G Li, Y Lan, J Qiao, M Bai, Z Wang, X Guo, D Ye, Z Jiapaer, Y
346   Yang, C Xia, G Wang, and J Kang. (2018). Long Noncoding RNA-1604 Orchestrates
347   Neural Differentiation through the miR-200c/ZEB Axis. Stem Cells **36**: 325-336.
348 12   Yin Y, P Yan, J Lu, G Song, Y Zhu, Z Li, Y Zhao, B Shen, X Huang, H Zhu, SH Orkin,
349   and X Shen. (2015). Opposing Roles for the lncRNA Haunt and Its Genomic Locus in
350   Regulating HOXA Gene Activation during Embryonic Stem Cell Differentiation. Cell
351   Stem Cell **16**: 504-16.
352 13   Yen YP, WF Hsieh, YY Tsai, YL Lu, ES Liau, HC Hsu, YC Chen, TC Liu, M Chang, J
353   Li, SP Lin, JH Hung, and JA Chen. (2018). Dlk1-Dio3 locus-derived lncRNAs perpetuate
354   postmitotic motor neuron cell fate and subtype identity. Elife **7**.
355 14   Thomson DW and ME Dinger. (2016). Endogenous microRNA sponges: evidence and
356   controversy. Nat Rev Genet **17**: 272-83.
357 15   Wobst H, B Schmitz, M Schachner, S Diestel, I Leshchyns'ka, and V Sytnyk. (2015).
358   Kinesin-1 promotes post-Golgi trafficking of NCAM140 and NCAM180 to the cell
359   surface. J Cell Sci **128**: 2816-29.
360 16   Lopez-Pajares V, K Qu, J Zhang, DE Webster, BC Barajas, Z Siprashvili, BJ Zarnegar,
361   LD Boxer, EJ Rios, S Tao, M Kretz, and PA Khavari. (2015). A LncRNA-MAF:MAFB

362   transcription factor network regulates epidermal differentiation. Dev Cell **32**: 693-706.

363   17   Ng SY, GK Bogu, BS Soh, and LW Stanton. (2013). The long noncoding RNA RMST
364   interacts with SOX2 to regulate neurogenesis. Mol Cell **51**: 349-59.

365   18   Wang P, Y Xue, Y Han, L Lin, C Wu, S Xu, Z Jiang, J Xu, Q Liu, and X Cao. (2014).
366   The STAT3-binding long noncoding RNA lnc-DC controls human dendritic cell
367   differentiation. Science **344**: 310-3.

368   19   Thomson JA, J Itskovitz-Eldor, SS Shapiro, MA Waknitz, JJ Swiergiel, VS Marshall, and
369   JM Jones. (1998). Embryonic stem cell lines derived from human blastocysts. Science
370   **282**: 1145-7.

371   20   Chambers I and SR Tomlinson. (2009). The transcriptional foundation of pluripotency.
372   Development **136**: 2311-22.

373   21   Wang Y, Z Xu, J Jiang, C Xu, J Kang, L Xiao, M Wu, J Xiong, X Guo, and H Liu.
374   (2013). Endogenous miRNA sponge lincRNA-RoR regulates Oct4, Nanog, and Sox2 in
375   human embryonic stem cell self-renewal. Dev Cell **25**: 69-80.

376   22   Zhang W, E Walker, OJ Tamplin, J Rossant, WL Stanford, and TR Hughes. (2006).
377   Zfp206 regulates ES cell gene expression and differentiation. Nucleic Acids Res **34**:
378   4780-90.

379   23   Wang ZX, CH Teh, JL Kueh, T Lufkin, P Robson, and LW Stanton. (2007). Oct4 and
380   Sox2 directly regulate expression of another pluripotency transcription factor, Zfp206, in
381   embryonic stem cells. J Biol Chem **282**: 12822-30.

382   24   Babaie Y, R Herwig, B Greber, TC Brink, W Wruck, D Groth, H Lehrach, T Burdon, and
383   J Adjaye. (2007). Analysis of Oct4-dependent transcriptional networks regulating self-
384   renewal and pluripotency in human embryonic stem cells. Stem Cells **25**: 500-10.

385   25   Dasen JS, BC Tice, S Brenner-Morton, and TM Jessell. (2005). A Hox regulatory
386   network establishes motor neuron pool identity and target-muscle connectivity. Cell **123**:
387   477-91.

388   26   Lacombe J, O Hanley, H Jung, P Philippidou, G Surmeli, J Grinstein, and JS Dasen.
389   (2013). Genetic and functional modularity of Hox activities in the specification of limb-
390   innervating motor neurons. PLoS Genet **9**: e1003184.

391   27   Jung H, J Lacombe, EO Mazzoni, KF Liem, Jr., J Grinstein, S Mahony, D
392   Mukhopadhyay, DK Gifford, RA Young, KV Anderson, H Wichterle, and JS Dasen.
393   (2010). Global control of motor neuron topography mediated by the repressive actions of
394   a single hox gene. Neuron **67**: 781-96.

395   28   Wu F, C Zhang, J Cai, F Yang, T Liang, X Yan, H Wang, W Wang, J Chen, and T Jiang.
396   (2017). Upregulation of long noncoding RNA HOXA-AS3 promotes tumor progression
397   and predicts poor prognosis in glioma. Oncotarget **8**: 53110-53123.

398   29   Gaufo GO, KR Thomas, and MR Capecchi. (2003). Hox3 genes coordinate mechanisms
399   of genetic suppression and activation in the generation of branchial and somatic
400   motoneurons. Development **130**: 5191-201.

401   30   Schubert M, ND Holland, V Laudet, and LZ Holland. (2006). A retinoic acid-Hox
402   hierarchy controls both anterior/posterior patterning and neuronal specification in the
403   developing central nervous system of the cephalochordate amphioxus. Dev Biol **296**:
404   190-202.

405   31   Chipman PH, M Schachner, and VF Rafuse. (2014). Presynaptic NCAM is required for
406   motor neurons to functionally expand their peripheral field of innervation in partially
407   denervated muscles. J Neurosci **34**: 10497-510.

408   32   Zhang L and F Ding. (2019). Hsa_circ_0008945 promoted breast cancer progression by
409   targeting miR-338-3p. Onco Targets Ther **12**: 6577-6589.
410

Primer sequences of five lncRNAs and mRNAs

Table 1 primer sequences of five lncRNAs and mRNAs

Gene	Forward	Reverse
GAPDH	GGAAGCTTGTCATCAATGGAAATC	TGATGACCCTTTTGGCTCCC
LncRNA rp11.001	CAGCCCAAGGAACATCTCACC	TCTTGCCAACTTGAGTGTCCAT
LncRNA rp11.003	ATCGGACTGTTCAACTCACCTG	TCAGCCGCTAAGCCAAGAAG
NCAM1-AS	TGAGATGCGAGACCTCCAGAC	CTCCAACTGCCTCATTATCCG
LncRNA rp11-c9-001	GGGGGCTGGAAACCAACTTAT	CATCCCAAGTCCAGCGTGAA
H19	CGGCCTTCCTGAACACCTTA	GTGTCTTTGATGTTGGGCTGATG
ZSCAN10	GCCACCGTTCCGCAATA	GCAGGTGTCGCAGCAGATT
CST1	CCCCAAGGAGGAGGATAGGAT	AGTTGGGCTGGGACTTGGTA
VRTN	TCCCGCTCAACCTACTATGCC	CGTTTGAAGCAGCGATAGGG
OCT4	TCTATTTGGGAAGGTATTCAGCC	CCTCTCACTCGGTTCTCGATACTG
HOXA3	CTCAGAATGCCAGCAACAACC	ACAGGTAGCGGTTGAAGTGGA
SP9	CCAAGCAGTTTTTCCGAGCAG	GGCTCGTGTTGCCGATCTT

Figure 1

Differentiation of hESCs into MNs

(A) Schematic diagram of the protocol used to obtain MNs from hESCs. hESCs, human embryonic stem cells; NEPs, neuroepithelial progenitors; MNPs, motor neuron progenitors; MNs, motor neurons. (B-D) hESCs differentiated to SOX1+ NEPs at day 6, OLIG2+ MNPs at day 12 and HB9+ MNs at day 18, respectively. Scale bar=50 μm.
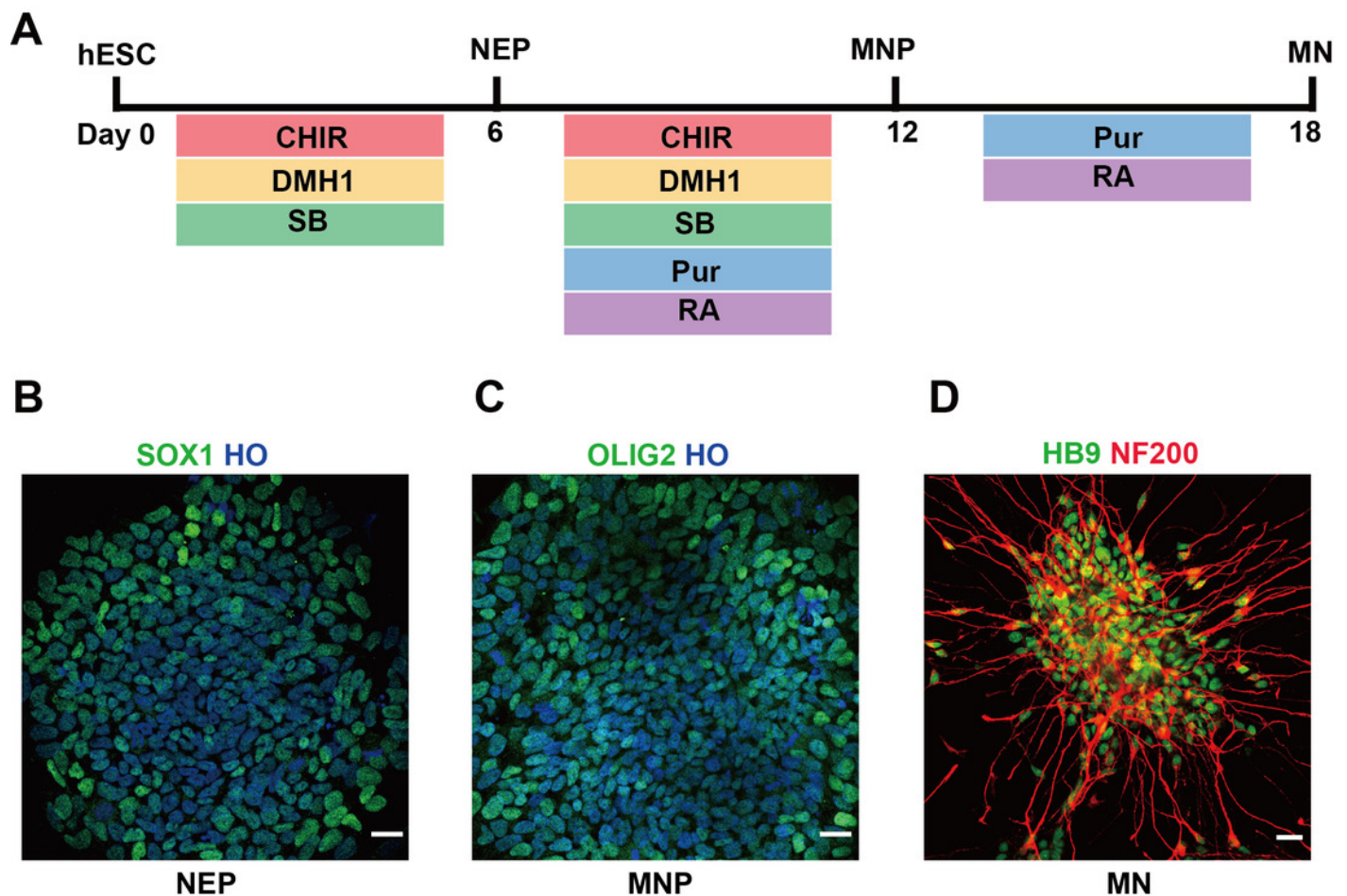
Figure 2

Expression Profiles of lncRNAs

(A-C) Plot indicated up-regulated and down-regulated lncRNAs at different stages points of MN differentiation from ESCs. (D-E) Venn diagram showed the number of overlap lncRNAs during the different stages of MN differentiation from ESCs.
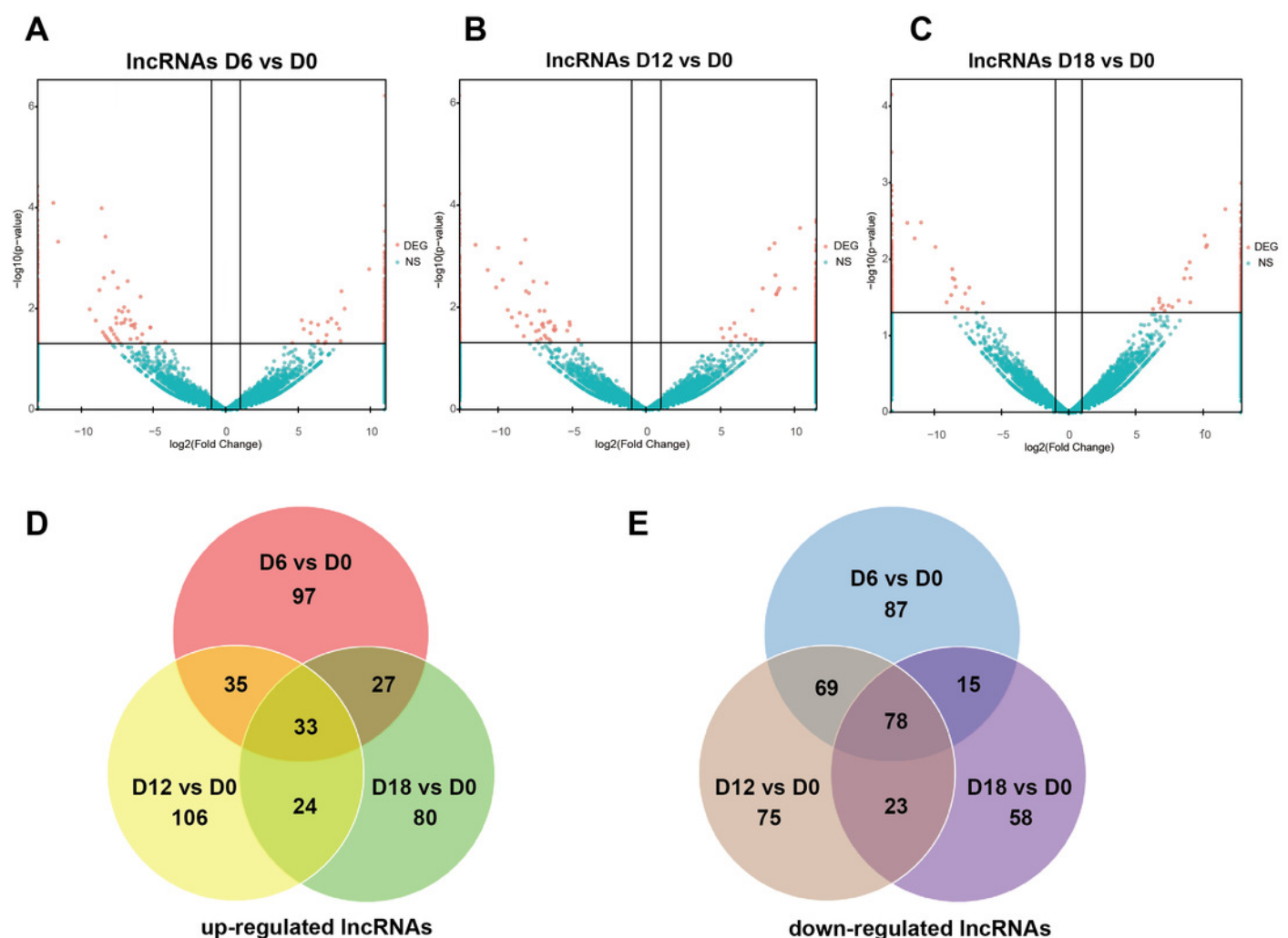
Figure 3

Expression Profiles of mRNAs

(A-C) Plot indicated up-regulated and down-regulated mRNAs at different stages points of MN differentiation from ESCs. (D-E) Venn diagram showed the number of overlap mRNAs during the different stages of MN differentiation from ESCs.
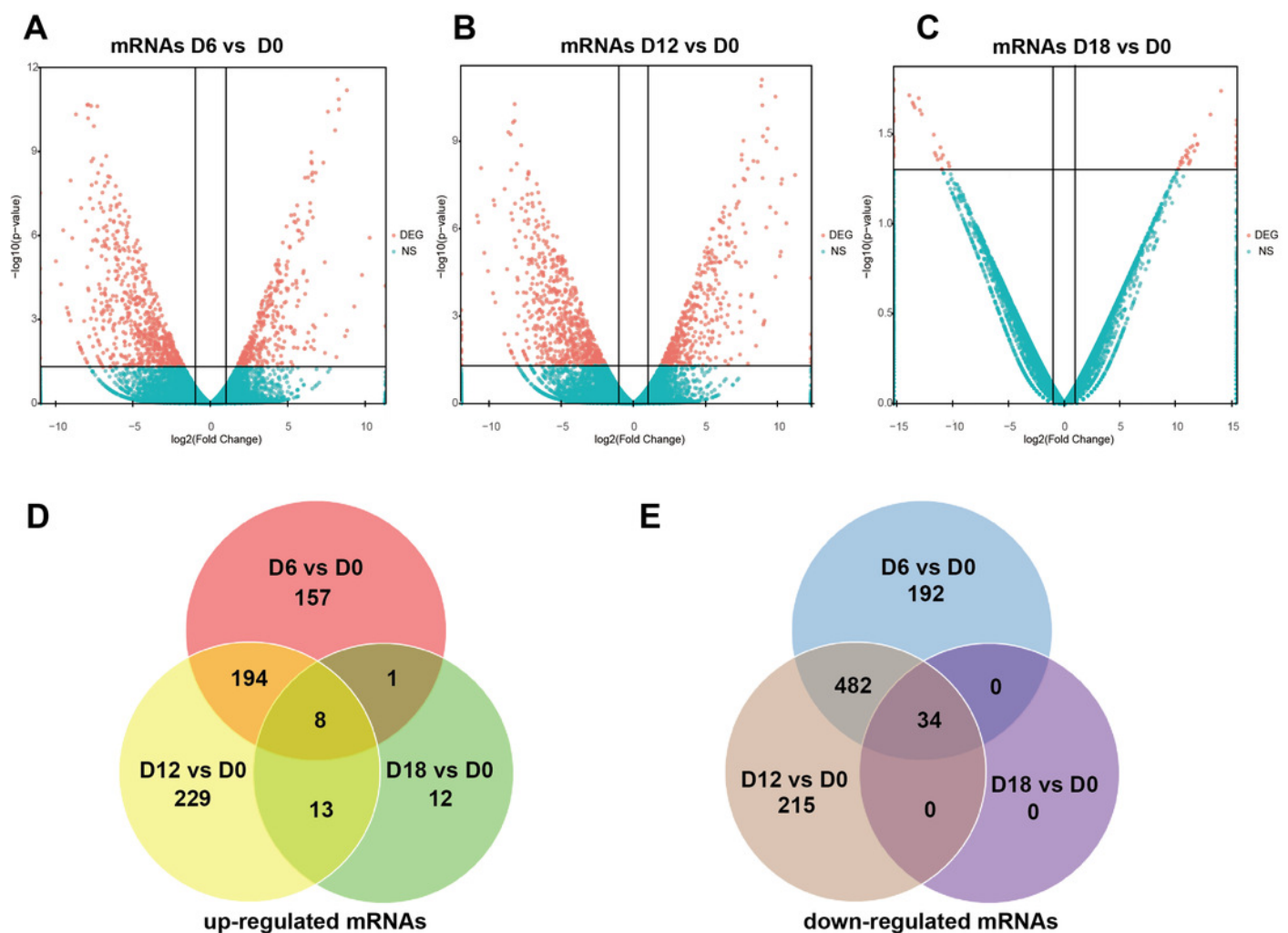
Figure 4

Validation of DElncRNAs and mRNAs in MN differentiation

(A-E) qRT-PCR analysis of the 5 DEmRNAs during MN differentiation. (F-J) qRT-PCR analysis of the 5 DElncRNAs up-regulated during MN differentiation * P < 0.05, ** P < 0.01, *** P < 0.001 and **** P < 0.0001 compared to D0. The number of each group was three to four.

A

OCT4

B

VRTN

C

ZSCAN10

D

SP9

E

HOXA3

F

LncRNA rp11.003

G

LncRNA rp11.001

H

LncRNA rp11-c9-001

I

LncRNA H19

J

LncRNA NCAM1
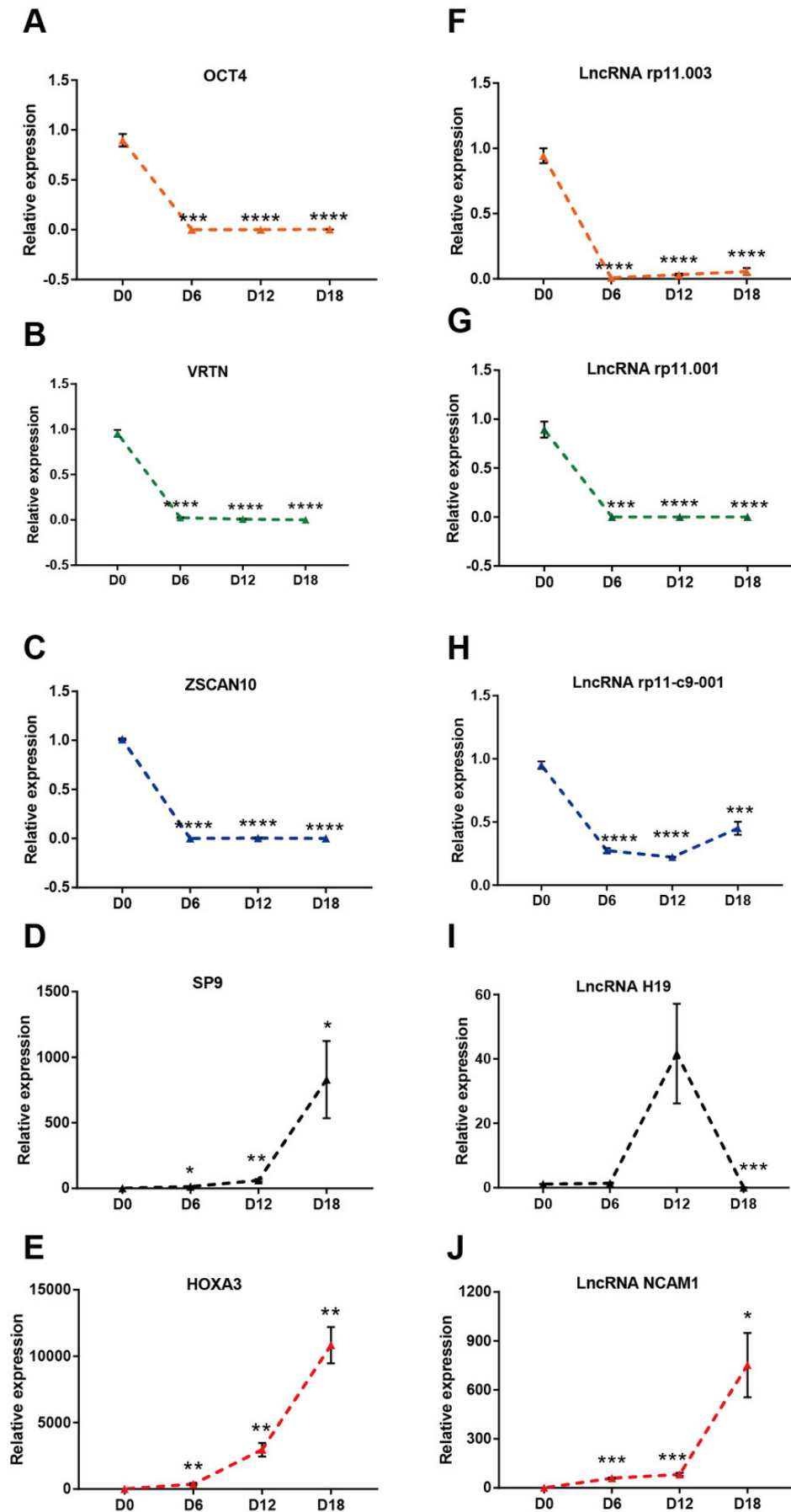
Figure 5

Bioinformatic analysis of DEmRNAs the biological function

(A) Go analysis of shared DEmRNAs at D6, D12 and D18 compared with D0. (B) Heat map of shared DEmRNAs at D6, D12 and D18 compared with D0. (C) Protein interaction network analysis of shared DE mRNAs at D6, D12 and D18 compared with D0.
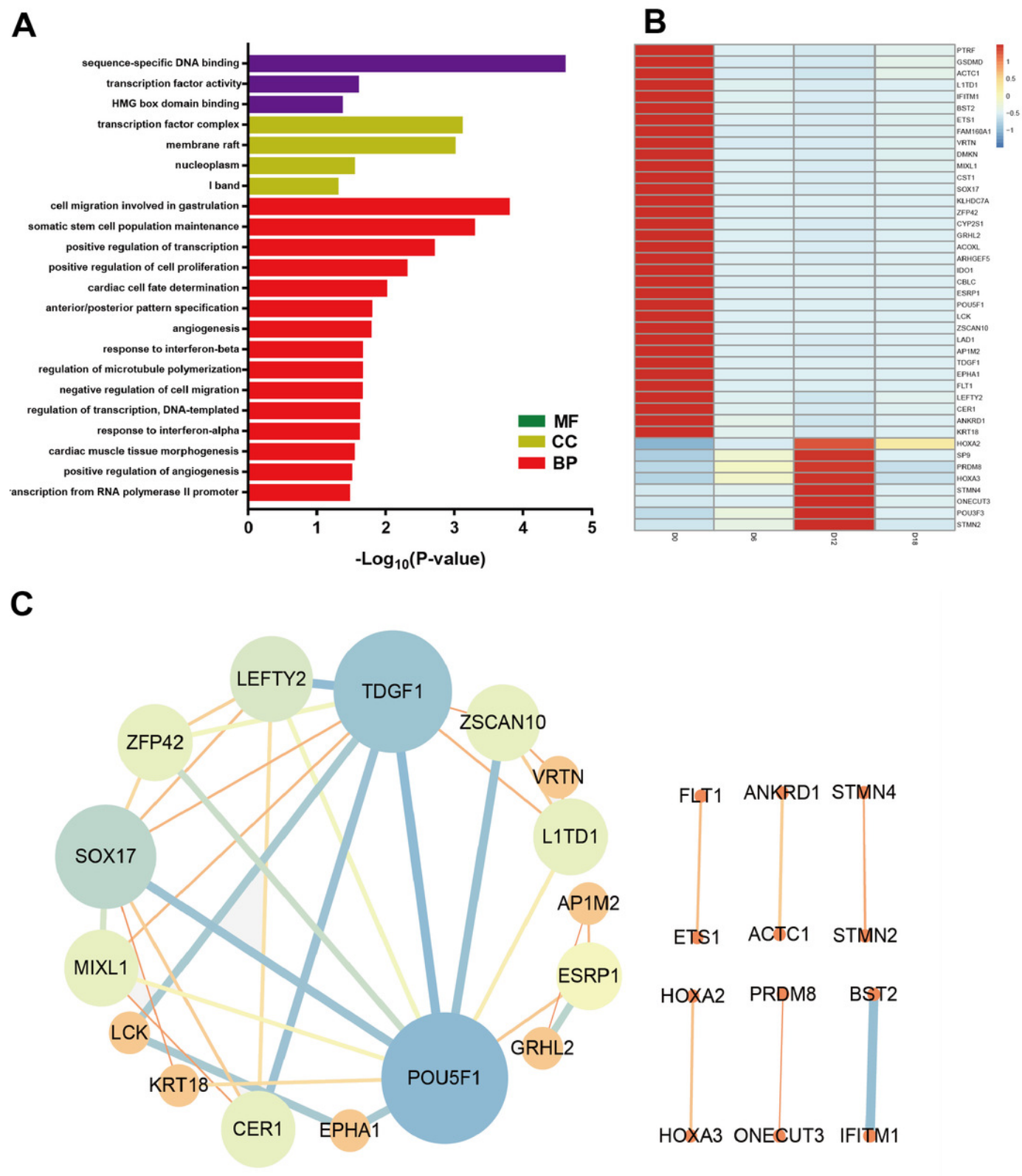
Figure 6

Bioinformatic analysis of DElncRNAs the biological function

(A) Go analysis of DElncRNAs at MN stage. (B) KEGG analysis of DElncRNAs at MN stage. (C) Veen diagram showed mRNAs tagerted by DElncRNA and DEmRNAs at MN stage.
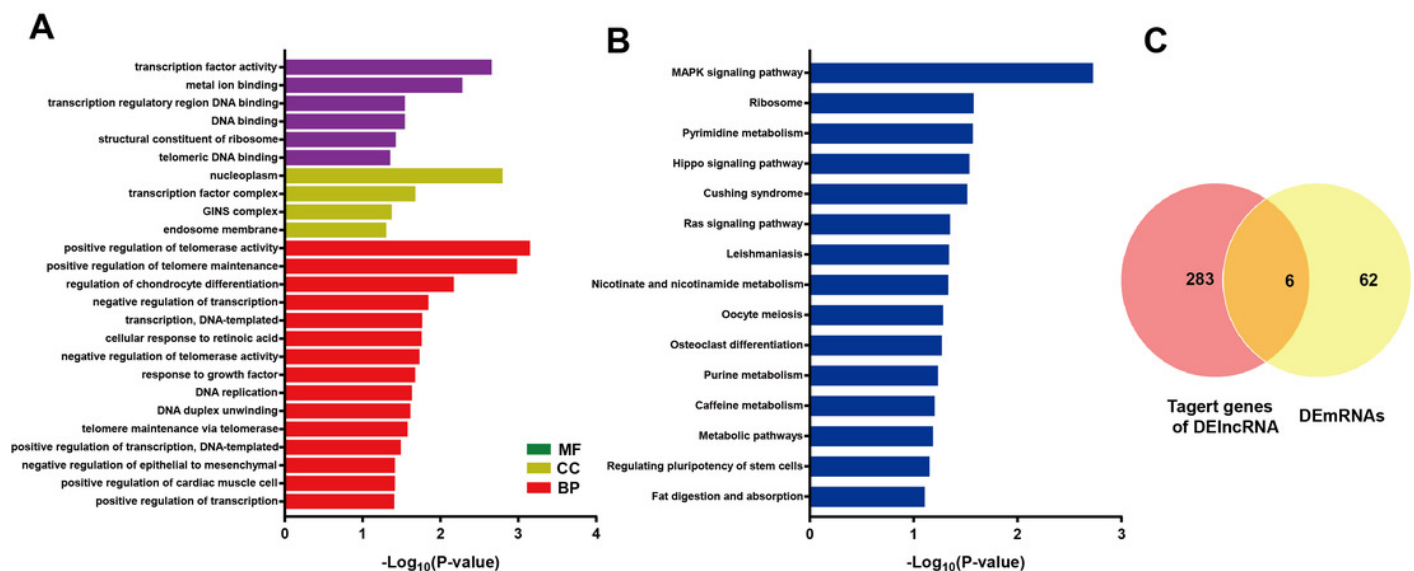
Figure 7

Protein interaction network analysis of mRNAs targeted by DElncRNAs at MN stage
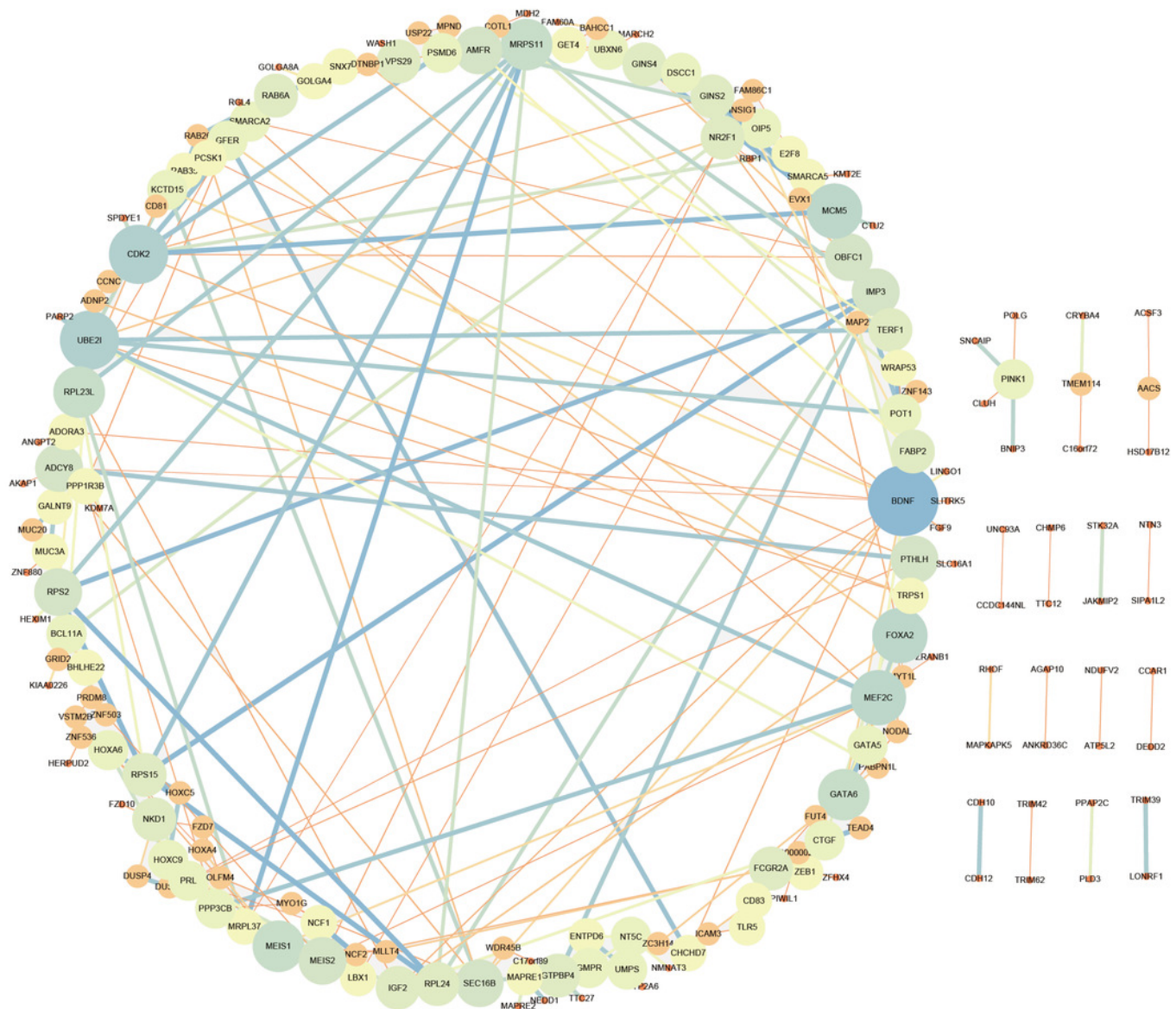
Figure 8

Figure 6. Silencing of lncRNA NCAM1-AS inhibit MNP differentiation.

(A) The expression of HOXA3 was analyzed after NCAM1-AS knockdown. (B) Immunostaining of OLIG2 expression in the after NCAM1-AS knockdown at MNP stage. Scare bar =50 μm. * P < 0.05, ** P < 0.01.